Electronic Supplementary Information (ESI)

Luminescence tuning and sensing properties of stable 2D lanthanide metal-organic frameworks built by symmetrical flexible tricarboxylic acid ligand containing ether oxygen bond

Jiao-Min Wang, Peng-Feng Zhang, Jian-Guo Cheng, Yao Wang, Lu-Lu Ma, Guo-Ping Yang, and Yao-Yu Wang*

Key Laboratory of Synthetic and Natural Functional Molecule of the Ministry of Education, Shaanxi Key Laboratory of Physico-Inorganic Chemistry, College of Chemistry & Materials Science, Northwest University, Xi'an 710127, P. R. China.

E-mail: wyaoyu@nwu.edu.cn

Contents

S1. Materials, devices and the crystal data characterization.

Table S1. Selected bond lengths (Å) and bond angles (deg) for complex **M-Eu**, **M-Tb** and **M-Dy**.

Table S2. Different molar ratio content of Eu^{3+} and Tb^{3+} in doped **M-Eu$_x$Tb$_{1-x}$**.

Table S3. The value of η_T for doped complex a, b, c, d, e, f, g and h.

Table S4. The quenching constants of the **M-Eu** and reported MOFs for detecting NB.

Fig. S1. IR spectra of **M-Ln**.

Fig. S2. The coordination geometry of Eu^{3+} in **M-Eu**.

Fig. S3. Graphic representation for the distorted AB motifs of **M-Eu.**

Fig. S4. Dished lines represent hydrogen bonds between the 2D layerered network and water molecules for **M-Eu**.

Fig. S5. PXRD patterns of **M-Ln**.

Fig. S6. PXRD patterns of bimetallic doped samples.

Fig. S7. TGA curve of **M-Ln**.

Fig. S8. PXRD of **M-Eu** by soaking through small molecules with different solvents.

Fig. S9. PXRD of **M-Eu** within the pH range of 1-12.

Fig. S10. Excitation spectra of **H_3L** (a), **M-Dy** (b), **M-Eu** (c) and **M-Tb** (d).

Fig. S11. Luminescence decay lifetimes of **M-Eu** (a) and **M-Tb** (b).

Fig. S12. (a) The linear plot between (I_0/I) - 1 vs concentration of NB at lower concertation; (b) UV-vis adsorption spectra of NB and H_3L in ethanol solution, and the excitation spectrum of **M-Eu** in ethanol solution.

Fig. S13. Cycle experiments of the fluorescence quenching of **M-Eu** by NB recovery after washing by ethanol for four times.

Fig. S14. PXRD patterns of M-Eu after cycling experiments on sensing NB.

S1. Materials, devices and the crystal data characterization.

Chemicals and Materials

The instrument of Bruker EQUINOX-55 FT-IR spectrometer provides the corresponding infrared spectra data. Elemental analysis was taken on a PerkinElmer 2400C elemental analyser to detect the content of carbon and hydrogen. Using the equipment called NETZSCH STA 449C to perform thermogravimetric analyses, temperature ranging from 30-800 °C under the nitrogen stream protection (the heating rate is 10 °C min^{-1}). The instrument named Edinburgh FLS920 fluorescence was applied to record the photoluminescence spectra for **M-Ln**. The device of FluoroMax-4 spectrophotometer was used to obtain the data of quantum efficiency. UV-visible spectrophotometer studies were performed on the device of Hitachi U-3310 spectrometer.

Single crystal data collection, refinement and performance characterization

The crystal data of **M-Ln** were obtained on a Bruker SMART APEX II diffractometer matched with CCD detector and Mo Kα radiation (λ = 0.71073 Å). The structures were refined using the *Olex2* program. Here, using a program named Shel XT for rough solution structure and then using the refine program to refine the structure in depth.[1,2] All non-H atoms were further refined through anisotropic thermal parameters, added at proper positions and refined with the riding models. After that all of the hydrogen atoms from the flexible ligands using the ideal hydrogenation method added at proper place. Free water and hydrogen on the coordination water were taken to Fourier hydrogenation. Also, the SQUEEZE command was adopted in the process of structural refinement,[3] squeezing the disordered solvent molecules in structures. But there is a B level alert of **M-Eu** was existed. In the structure of **M-Eu**, when this peak was designated as the atom, the next refinement leads to a very high Uiso value of beyond 1. Therefore, it can be inferred that this peak should be a ghost peak, which is not part of the crystal structure. It is may be caused by the strong diffraction intensity during the collection of single crystal data. Hence, a B level alter although presented in the CIF file, it will not affect the whole crystal structure and the property of **M-Eu**. The final molecular formula of **M-Ln** was confirmed through using the data of single crystal structure data, TGA, FT-IR and element analysis. Related crystal data for **M-Ln** is listed in Table 1, selected bond distances/angles are shown in Table S1. CCDC numbers are 1972129–1972131, corresponding to **M-Eu**, **M-Tb** and **M-Dy**.

Table S1. Selected bond lengths (Å) and bond angles (deg) for complex **M-Eu**, **M-Tb** and **M-Dy**.

M-Eu			
Eu(1)-O(1)	2.354(2)	Eu(1)-O(2)#1	2.354(3)
Eu(1)-O(4)#2	2.359(3)	Eu(1)-O(3)#3	2.350(3)
Eu(1)-O(5)#4	2.345(3)	Eu(1)-O(6)#5	2.351(3)
Eu(1)-O(8)	2.502(3)	Eu(1)-O(7)	2.595(3)
O(2)-Eu(1)#1	2.354(3)	O(4)-Eu(1)#2	2.359(3)
O(3)-Eu(1)#6	2.350(3)	O(5)-Eu(1)#7	2.345(3)
O(6)-Eu(1)#8	2.351(3)		
O(1)-Eu(1)-O(2)#1	90.66(9)	O(1)-Eu(1)-O(4)#2	144.65(11)
O(1)-Eu(1)-O(8)	73.42(11)	O(1)-Eu(1)-O(7)	68.02(9)
O(2)#1-Eu(1)-O(4)#2	84.81(10)	O(2)#1-Eu(1)-O(8)	73.88(11)

O(2)#1-Eu(1)-O(7)	68.31(9)	O(4)#2-Eu(1)-O(8)	71.64(11)
O(4)#2-Eu(1)-O(7)	139.57(9)	O(3)#3-Eu(1)-O(1)	85.29(11)
O(3)#3-Eu(1)-O(2)#1	143.50(11)	O(3)#3-Eu(1)-O(4)#2	118.05(13)
O(3)#3-Eu(1)-O(6)#5	71.36(11)	O(3)#3-Eu(1)-O(8)	138.00(12)
O(3)#3-Eu(1)-O(7)	76.62(10)	O(5)#4-Eu(1)-O(1)	142.98(11)
O(5)#4-Eu(1)-O(2)#1	85.14(11)	O(5)#4-Eu(1)-O(4)#2	71.63(11)
O(5)#4-Eu(1)-O(3)#3	76.91(11)	O(5)#4-Eu(1)-O(6)#5	117.40(12)
O(5)#4-Eu(1)-O(8)	138.93(12)	O(5)#4-Eu(1)-O(7)	76.33(10)
O(6)#5-Eu(1)-O(1)	86.07(10)	O(6)#5-Eu(1)-O(2)#1	144.62(11)
O(6)#5-Eu(1)-O(4)#2	77.98(11)	O(6)#5-Eu(1)-O(8)	71.43(11)
O(6)#5-Eu(1)-O(7)	140.15(9)	O(8)-Eu(1)-O(7)	124.45(8)
C(1)-O(1)-Eu(1)	145.0(3)	C(1)-O(2)-Eu(1)#1	147.1(3)
M-Tb			
Tb(1)-O(1)#1	2.3401(19)	Tb(1)-O(2)#2	2.3260(19)
Tb(1)-O(5)#3	2.3139(18)	Tb(1)-O(6)#4	2.3237(17)
Tb(1)-O(7)#5	2.3475(19)	Tb(1)-O(8)	2.3195(19)
Tb(1)-O(9)	2.474(2)	Tb(1)-O(10)	2.5674(19)
O(1)-Tb(1)#6	2.3401(19)	O(2)-Tb(1)#2	2.3260(19)
O(3)-C(13)	1.372(3)	O(5)-Tb(1)#7	2.3139(18)
O(6)-Tb(1)#5	2.3238(17)	O(7)-Tb(1)#4	2.3476(19)
O(1)#1-Tb(1)-O(7)#5	77.21(7)	O(6)#4-Tb(1)-O(2)#2	84.80(7)
O(1)#1-Tb(1)-O(9)	72.60(8)	O(6)#4-Tb(1)-O(7)#5	80.17(7)
O(1)#1-Tb(1)-O(10)	142.05(7)	O(6)#4-Tb(1)-O(9)	78.15(8)
O(2)#2-Tb(1)-O(1)#1	109.87(8)	O(6)#4-Tb(1)-O(10)	68.26(6)
O(2)#2-Tb(1)-O(7)#5	72.41(7)	O(7)#5-Tb(1)-O(9)	71.28(8)
O(2)#2-Tb(1)-O(9)	141.93(8)	O(7)#5-Tb(1)-O(10)	137.62(6)
O(2)#2-Tb(1)-O(10)	77.11(7)	O(8)-Tb(1)-O(1)#1	70.25(8)
O(5)#3-Tb(1)-O(1)#1	91.30(7)	O(8)-Tb(1)-O(2)#2	77.39(7)
O(5)#3-Tb(1)-O(2)#2	142.71(7)	O(8)-Tb(1)-O(6)#4	142.30(7)
O(5)#3-Tb(1)-O(6)#4	93.48(7)	O(8)-Tb(1)-O(7)#5	123.92(8)
O(5)#3-Tb(1)-O(7)#5	144.05(7)	O(8)-Tb(1)-O(9)	133.96(8)
O(5)#3-Tb(1)-O(8)	81.79(8)	O(8)-Tb(1)-O(10)	75.45(7)
O(5)#3-Tb(1)-O(9)	72.78(8)	O(9)-Tb(1)-O(10)	125.34(6)
O(5)#3-Tb(1)-O(10)	67.83(6)	C(22)-O(1)-Tb(1)#6	165.93(19)
O(6)#4-Tb(1)-O(1)#1	147.44(7)	C(22)-O(2)-Tb(1)#2	145.49(18)
M-Dy			
Dy(01)-O(1)#1	2.335(2)	Dy(01)-O(10)	2.466(3)
Dy(01)-O(2)#2	2.305(2)	O(1)-Dy(01)#1	2.335(2)
Dy(01)-O(5)#3	2.313(3)	O(2)-Dy(01)#6	2.305(2)
Dy(01)-O(6)	2.299(2)	O(5)-Dy(01)#3	2.313(3)
Dy(01)-O(7)#4	2.309(2)	O(7)-Dy(01)#7	2.309(2)
Dy(01)-O(8)#5	2.331(2)	O(8)-Dy(01)#8	2.331(2)
Dy(01)-O(9)	2.557(2)		
O(1)#1-Dy(01)-O(9)	137.86(8)	O(6)-Dy(01)-O(7)#4	142.88(9)

O(1)#1-Dy(01)-O(10)	71.29(10)	O(6)-Dy(01)-O(8)#5	91.13(9)
O(2)#2-Dy(01)-(1)#1	123.76(11)	O(6)-Dy(01)-O(9)	67.95(8)
O(2)#2-Dy(01)-(5)#3	142.25(10)	O(6)-Dy(01)-O(10)	72.72(10)
O(2)#2-Dy(01)-(7)#4	77.26(9)	O(7)#4-Dy(01)-(1)#1	72.40(10)
O(2)#2-Dy(01)-(8)#5	70.46(10)	O(7)#4-Dy(01)-(5)#3	84.99(10)
O(2)#2-Dy(01)-O(9)	75.27(9)	O(7)#4-Dy(01)-(8)#5	109.83(10)
O(2)#2-Dy(01)-O(10)	134.12(11)	O(7)#4-Dy(01)-O(9)	77.20(9)
O(5)#3-Dy(01)-(1)#1	80.40(9)	O(7)#4-Dy(01)-O(10)	141.89(10)
O(5)#3-Dy(01)-(8)#5	147.29(10)	O(8)#5-Dy(01)-(1)#1	76.96(9)
O(5)#3-Dy(01)-O(9)	68.38(9)	O(8)#5-Dy(01)-O(9)	142.03(8)
O(5)#3-Dy(01)-O(10)	78.01(10)	O(8)#5-Dy(01)-O(10)	72.55(10)
O(6)-Dy(01)-O(1)#1	143.98(9)	O(10)-Dy(01)-O(9)	125.36(8)
O(6)-Dy(01)-O(2)#2	81.80(10)	C(1)-O(1)-Dy(01)#1	156.6(2)
O(6)-Dy(01)-O(5)#3	93.53(9)	C(1)-O(2)-Dy(01)#6	160.2(2)

Symmetry codes: **M-Eu**: #1 -x,-y,-z; #2 -x,-y+1,-z; #3 x,-y+1/2,z+1/2; #4 -x,y+1/2,-z+1/2; #5 x,y+1,z; #6 x,-y+1/2,z-1/2; #7 -x,y-1/2,-z+1/2; #8 x,y-1,z. **M-Tb:** #1 x,-y+3/2,z-1/2; #2 -x+1,-y+1,-z+1; #3 x,-y+1/2, z-1/2; #4 -x+1,y-1/2,-z+1/2; #5 -x+1,y+1/2,-z+1/2; #6 x,-y+3/2,z+1/2; #7 x,-y+1/2,z+1/2. **M-Dy:** #1 -x+1,-y+2,-z+1; #2 x,-y+3/2,z-1/2; #3 -x+1,-y+1,-z+1; #4 -x+1,y+1/2,-z+1/2; #5 x,y+1,z; #6 x,-y+3/2,z+1/2; #7 -x+1,y-1/2,-z+1/2; #8 x,y-1,z.

Table S2. Different molar ratio content of Eu^{3+} and Tb^{3+} in doped **M-Eu$_x$Tb$_{1-x}$**.

	a	b	c	d	e	f	g
Eu^{3+}	0.1000	0.0588	0.0400	0.0333	0.0286	0.0256	0.0233
Tb^{3+}	0.9000	0.9412	0.0600	0.9667	0.9714	0.9744	0.9767

Table S3. The value of η_T for doped complex a, b, c, d, e, f, g and h.

Compound	τ (μs)	η_T
a	589.38	0.285756
b	522.66	0.366611
c	468.49	0.432257
d	440.73	0.465898
e	424.70	0.485324
f	409.44	0.503817
g	402.28	0.512494

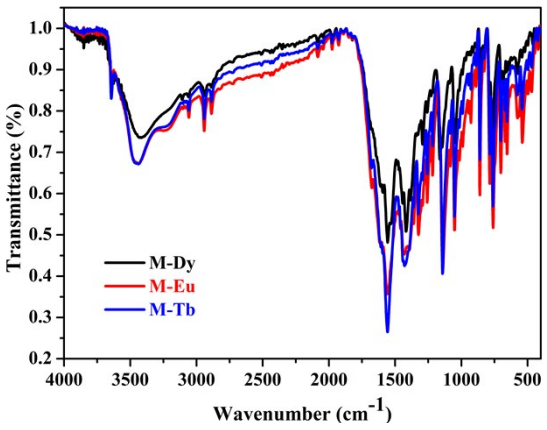

Fig. S1. IR spectra of **M-Ln**.

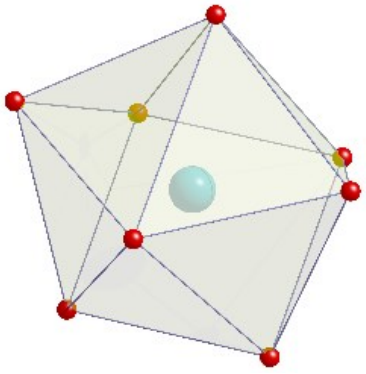

Fig. S2. The coordination geometry of Eu^{3+} in **M-Eu**.

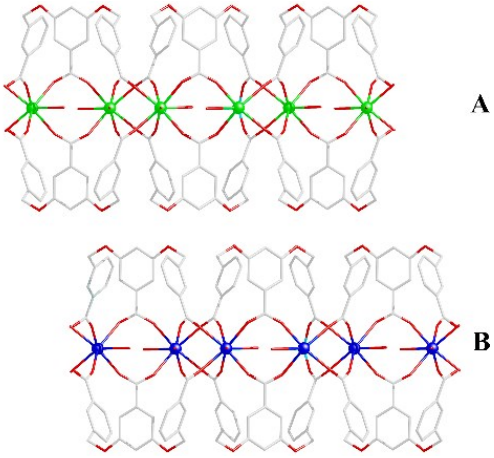

Fig. S3. Graphic representation for the distorted AB motifs of **M-Eu.**

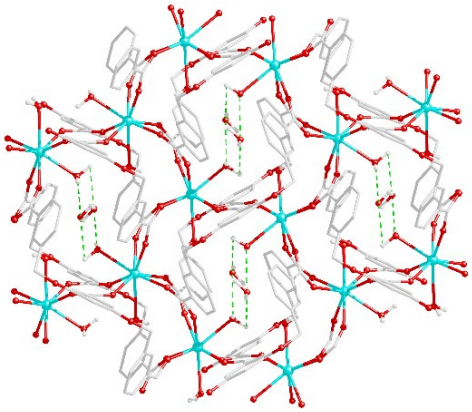

Fig. S4. Dished lines represent hydrogen bonds between the 2D layerered network and water molecules for **M-Eu**.

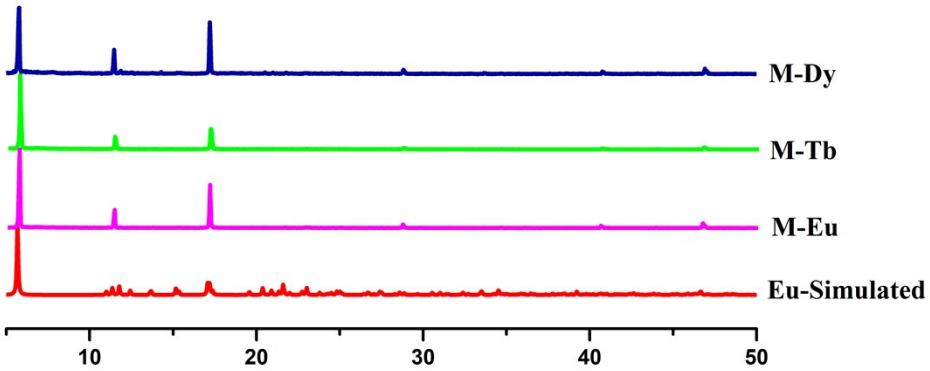

Fig. S5. PXRD patterns of **M-Ln**.

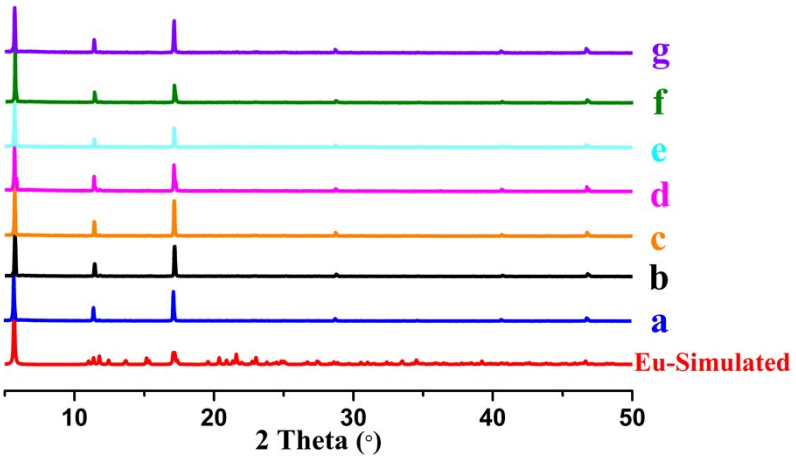

Fig. S6. PXRD patterns of bimetallic doped samples.

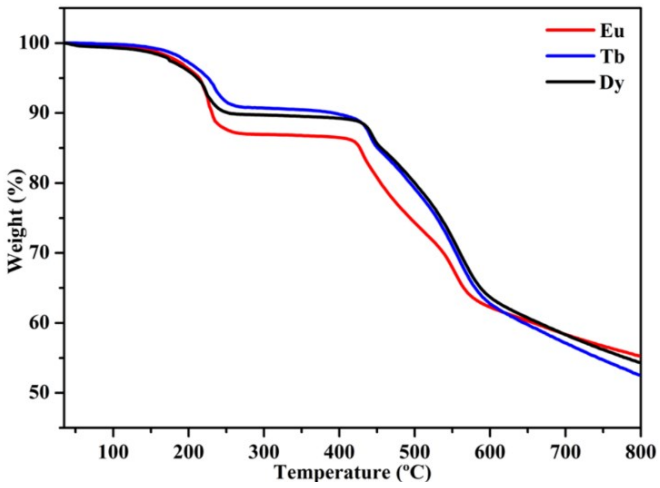

Fig. S7. TGA curve of **M-Ln**.

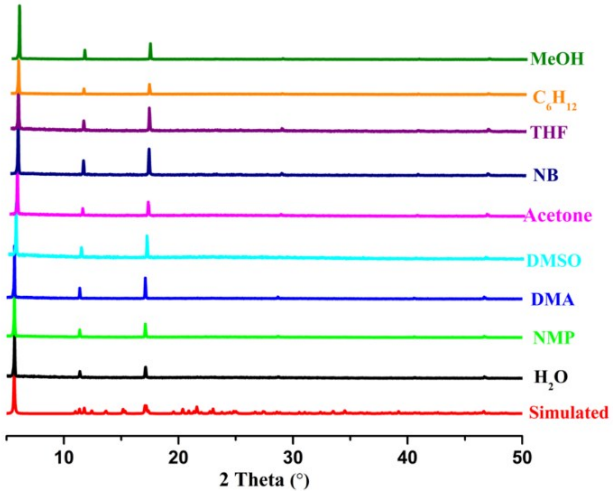

Fig. S8. PXRD of **M-Eu** by soaking through small molecules with different solvents.

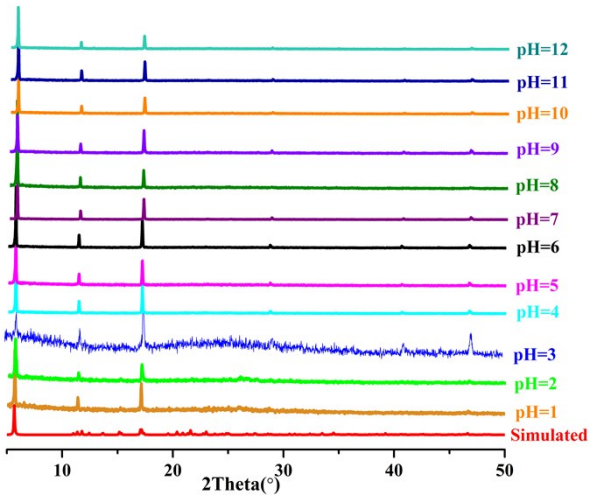

Fig. S9. PXRD of **M-Eu** within the range of 1-12 pH.

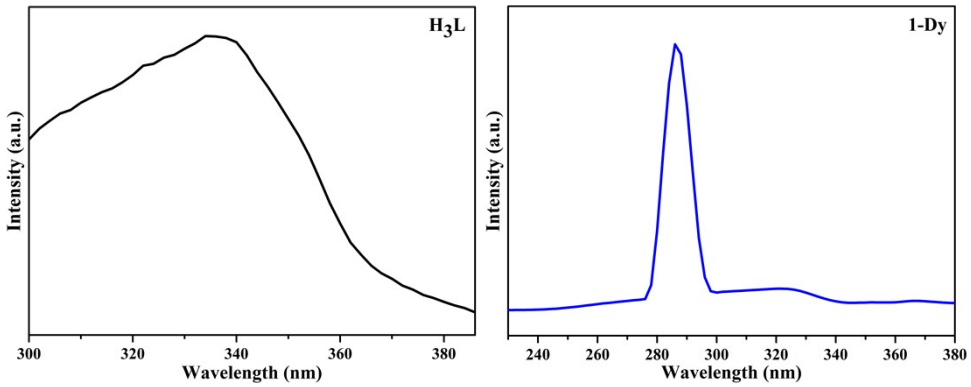

(a)

(b)

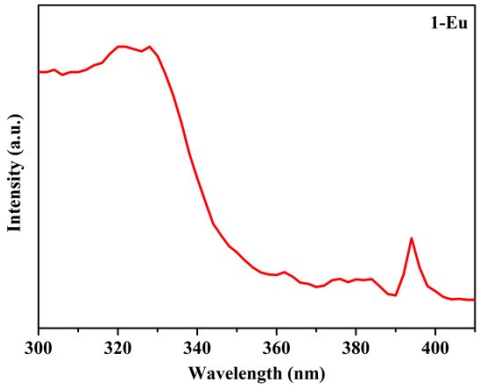

(c)

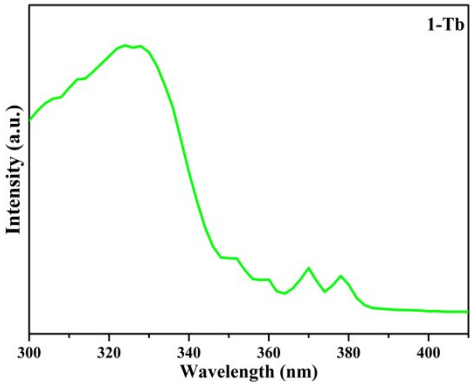

(d)

Fig. S10. Excitation spectra of **H_3L** (a), **M-Dy** (b), **M-Eu** (c) and **M-Tb** (d).

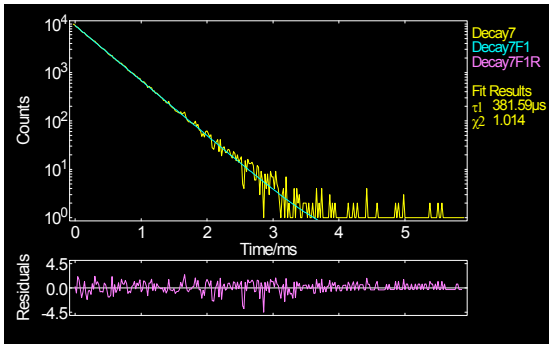

(a)

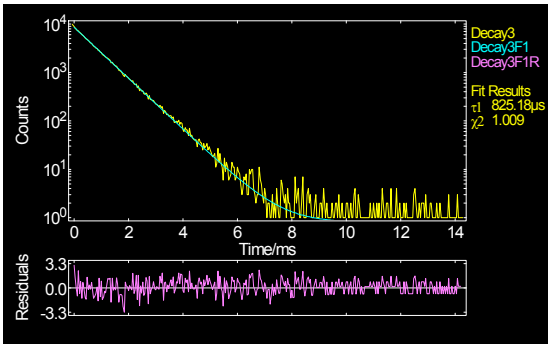

(b)

Fig. S11. Luminescence decay lifetimes of **M-Eu** (a) and **M-Tb** (b).

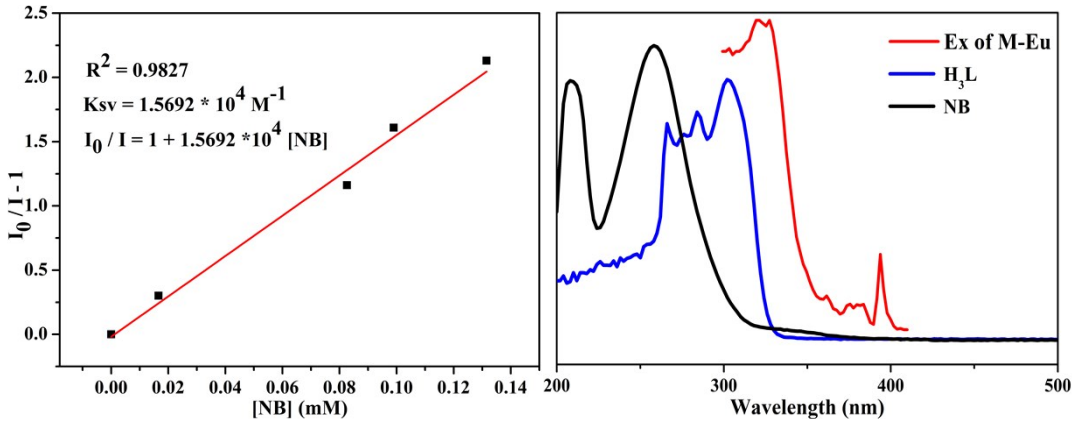

(a) (b)

Fig. S12. (a) The linear plot between (I_0 / I) - 1 vs concentration of NB at lower concertation; (b) UV-vis adsorption spectra of NB and H_3L in ethanol solution, and the excitation spectrum of **M-Eu** in ethanol solution.

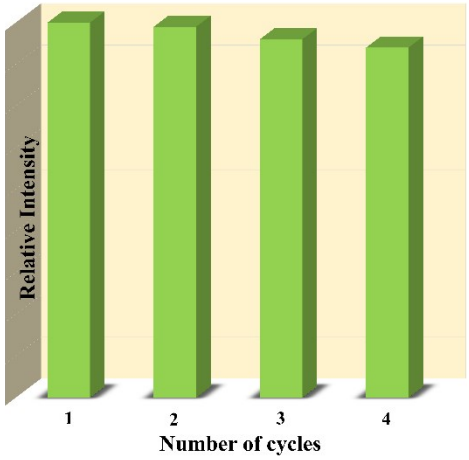

Fig. S13. Cycle experiments of the fluorescence quenching of **M-Eu** by NB recovery after washing by ethanol for four times.

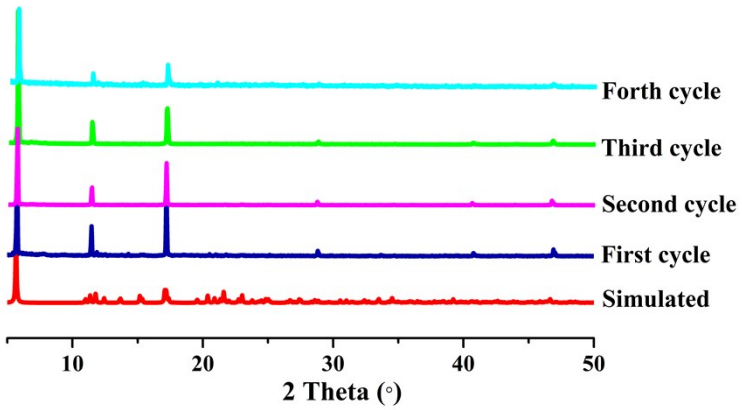

Fig. S14. PXRD patterns of **M-Eu** after cycling experiments on sensing NB.

Table S4. The quenching constants of the **M-Eu** and reported MOFs for detecting NB.

Molecular Formula	Quenching Constants (K_{SV})	Ref.
{[Eu(L)(H_2O)$_2$]·H_2O}$_n$	1.5692 × 104 M^{-1}	This work

$Eu_2Ti_4(\mu_2\text{-}O)_2(\mu_3\text{-}O)_4(phen)_2(tbza)_{10}\cdot 4CH_3CN$	0.095 ppm^{-1}	4
$\{[Eu_2(L_2)_2(H_2O)_5]\cdot 3H_2O\}_n$	1323 M^{-1}	5
$[Zn_4(L)_3O]\cdot 8DMF\cdot H_2O$	1.5479×10^2 M^{-1}	6
LPCMP1	89 M^{-1}	7
$\{[Cd_2(L)(DMA)]\cdot[H_2N(Me)_2]\}_n$	2.7×10^3 M^{-1}	8
$\{[Cd_{12}(Trz)_8(DMF)_2(H2O)_4](BDC)_9\}\cdot 2(Me_2NH_2)\cdot 4DMF\cdot 16H_2O$	35 M^{-1}	9

References

1 (a) G. M. Sheldrick, *SHELXL-97, program for the refinement of the crystal structures*, University of Göttingen, Germany, 1997. (b) G. M. Muller-Buschbaum, Crystal structure refinement with SHELXL, *Acta Crystallogr*, Sect. *C: Struct. Chem*., 2015, **71**, 3-8.

2 O. V. Dolomanov, L. J. Bourhis, R. J. Gildea, J. A. K. Howard and H. Puschmann, *J. Appl. Cryst*., 2009, **42**, 339-341.

3 L. Xu, J. Wang, Y. Xu, Z. Zhang, P. Lu, M. Fang, S. Li, P. Sun and H. K. Liu, *CrystEngComm*, 2014, **16**, 8656.

4 H. Zheng, Y. K. Deng, M. Y. Ye, Q. F. Xu, X. J. Kong, L. S. Long and L. S. Zheng, *Inorg. Chem*., 2020, **59**, 12404-12409.

5 Z. Sun, J. Sun, L. Xi, J. Xie, X. Wang, Y. Ma and L. Li, *Cryst. Growth Des*, 2020, **20**, 5225-5234.

6 D. Wu, J. Liu, J. Jin, J. Cheng, M. Wang, G. Yang and Y.-Y. Wang, *Cryst. Growth Des*., 2019, **19**, 6774-6783.

7 L. Pan, Z. Liu, M. Tian, B. C. Schroeder, A. E. Aliev and C. F. J. Faul, *ACS Appl. Mater. Interfaces*, 2019, **11**, 48352-48362.

8 Y.-T. Yan, J. Liu, G.-P. Yang, F. Zhang, Y.-K. Fan, W.-Y. Zhang and Y.-Y. Wang, *CrystEngComm*, 2018, **20**, 477-486.

9 Y. Chen, Z. Li, Q. Liu, Y. Shen, X. Wu, D. Xu, X. Ma, L. Wang, Q.-H. Chen, Z. Zhang and S. Xiang, *Cryst. Growth Des*., 2015, **15**, 3847-3852.